

Two Novel Classes of Enzymes Are Required for the Biosynthesis of Aurofusarin in *Fusarium graminearum**[§]

Received for publication, August 29, 2010, and in revised form, February 4, 2011. Published, JBC Papers in Press, February 4, 2011, DOI 10.1074/jbc.M110.179853

Rasmus J. N. Frandsen^{†§1}, Claes Schütt[¶], Birgitte W. Lund[¶], Dan Staerk[¶], John Nielsen[¶], Stefan Olsson[‡], and Henriette Giese^{||}

From the [†]Department of Agriculture and Ecology, Faculty of Life Sciences, University of Copenhagen, DK-1870 Frederiksberg, the [§]Center for Microbial Biotechnology, Department of Systems Biology, Technical University of Denmark, DK-2800 Kongens Lyngby, the [¶]Department of Basic Sciences and Environment, Faculty of Life Sciences, University of Copenhagen, DK-1870 Frederiksberg, and the ^{||}Faculty of Agricultural Sciences, University of Aarhus, 8000 Aarhus, Denmark

Previous studies have reported the functional characterization of 9 out of 11 genes found in the gene cluster responsible for biosynthesis of the polyketide pigment aurofusarin in *Fusarium graminearum*. Here we reanalyze the function of a putative aurofusarin pump (AurT) and the two remaining orphan genes, *aurZ* and *aurS*. Targeted gene replacement of *aurZ* resulted in the discovery that the compound YWA1, rather than nor-rubrofusarin, is the primary product of *F. graminearum* polyketide synthase 12 (FgPKS12). AurZ is the first representative of a novel class of dehydratases that act on hydroxylated γ -pyrones. Replacement of the *aurS* gene resulted in accumulation of rubrofusarin, an intermediate that also accumulates when the *GIP1*, *aurF*, or *aurO* genes in the aurofusarin cluster are deleted. Based on the shared phenotype and predicted subcellular localization, we propose that AurS is a member of an extracellular enzyme complex (GIP1-AurF-AurO-AurS) responsible for converting rubrofusarin into aurofusarin. This implies that rubrofusarin, rather than aurofusarin, is pumped across the plasma membrane. Replacement of the putative aurofusarin pump *aurT* increased the rubrofusarin-to-aurofusarin ratio, supporting that rubrofusarin is normally pumped across the plasma membrane. These results provide functional information on two novel classes of proteins and their contribution to polyketide pigment biosynthesis.

The plant pathogenic fungus *Fusarium graminearum* (teleomorph *Gibberella zeae*) is capable of producing a plethora of secondary metabolites, many of which belong to the polyketide class of compounds, such as the mycotoxins zearalenone, fusarin C, and aurofusarin (1). The *F. graminearum* genome encodes 15 polyketide synthases (PKS)² (2, 3), of which FgPKS12 is the progenitor of nor-rubrofusarin/rubrofusarin/aurofusarin

(4, 5), FgPKS4 and FgPKS13 are the progenitors of zearalenone (1, 6), FgPKS10 is the progenitor of fusarin C (7, 8), and FgPKS3 is the progenitor of an uncharacterized black/purple perithecial pigment (8). PKS genes are typically found in gene clusters that comprise genes encoding transcription factor, transporters, and tailoring enzymes required for biosynthesis of the final product (1, 4–6). In addition to genes encoding well characterized classes of enzymes, the clusters typically also include orphan genes that encode proteins annotated as “hypothetical” or “conserved hypothetical proteins,” signifying that no similarity to any previously characterized protein has been found. In the case of *F. graminearum*, more than half of all gene models found in the *Fusarium graminearum* Genome Database from the Munich Information Center for Protein Sequences (MIPS) fall into either of these two categories (9).

Functional characterization of hypothetical proteins is challenging, but those belonging to secondary metabolite gene clusters provide a unique opportunity because their location suggests a function in the respective biosynthetic pathways. The *PKS12* gene cluster in *F. graminearum*, which is responsible for biosynthesis of the red mycelium pigment aurofusarin (4, 10), consists of 11 co-regulated genes. Nine of these have been functionally characterized, all encoding well described classes of enzymes such as laccases (GIP1 and AurL2), polyketide synthase (PKS12), monooxygenase (AurF), *O*-methyltransferase (AurJ), oxidoreductase (AurO), major facilitator pump (AurT), and transcription factors (AurR1 and AurR2) (5, 11). However, the gene cluster also includes two genes, *aurZ* (FG02325) and *aurS* (FG02329), annotated as encoding “hypothetical proteins.” They are both regulated by the cluster-specific transcription factor AurR1, and their expression coincides with the remaining genes in the cluster (5), suggesting that they play a role in aurofusarin biosynthesis.

In the present study, we wish to gain a fuller understanding of the aurofusarin pathway and assign functions to the two hypothetical proteins, AurZ and AurS. The role of the putative aurofusarin pump (AurT) is reassessed, and a new hypothesis for the aurofusarin biosynthetic pathway is presented.

EXPERIMENTAL PROCEDURES

Bioinformatics—Sequences were retrieved from the genetic sequence database (GenBankTM) from the National Center for Biotechnology Information, the *Fusarium* Comparative Database from Broad Institute, and the MIPS *Fusarium*

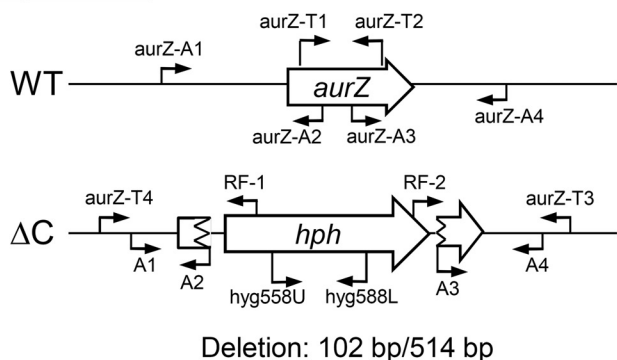
* This work was supported by a grant from the Danish Ministry for Food, Agriculture and Fisheries and by The Danish Research Council for Technology and Production Sciences (Grant 274-06-0371).

[§] The on-line version of this article (available at <http://www.jbc.org>) contains supplemental Figs. S1–S6 and Tables S1 and S2.

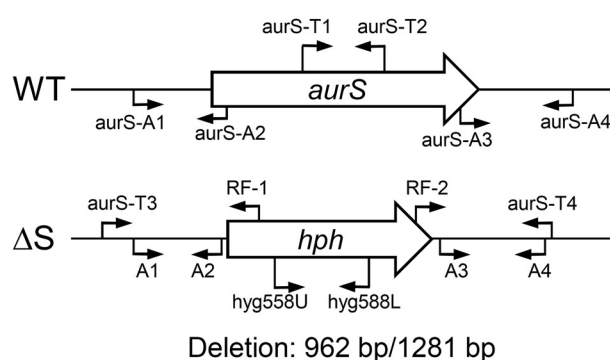
¹ To whom correspondence should be addressed: Center for Microbial Biotechnology, Dept. of Systems Biology, Technical University of Denmark, Soltofts Plads, 2800 Kongens Lyngby, Denmark. Tel.: 45-4525-2708; Fax: 45-4588-4148; E-mail: rasf@bio.dtu.dk.

² The abbreviations used are: PKS, polyketide synthase; HPLC-DAD, high-performance liquid chromatography-diode array detection; aa, amino acid; SD, scytalone dehydratase.

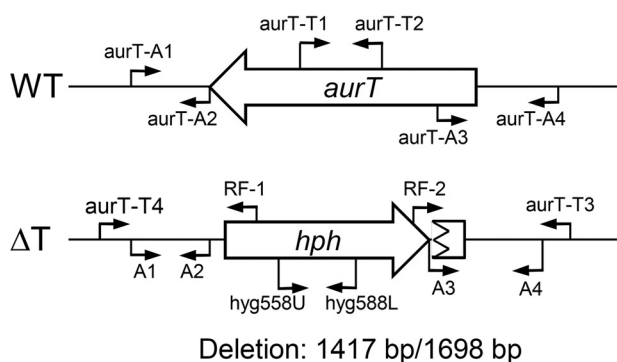
A) $\Delta aurZ$



B) $\Delta aurS$



C) $\Delta aurT$



D) $\Delta aurZ/J$

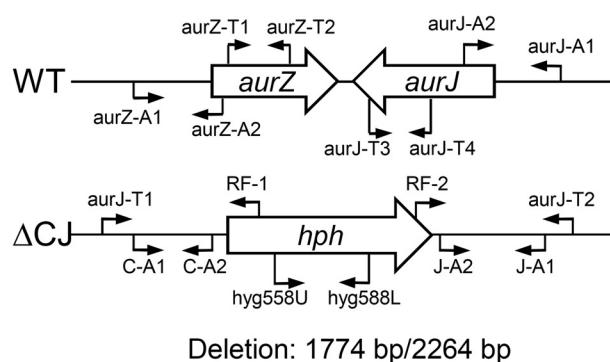


FIGURE 1. **Strategy for genetic modifications.** A–D, construction of targeted gene replacement strains and placement of primers for verification of the strains: A, $\Delta aurZ$; B, $\Delta aurS$; C, $\Delta aurT$; D, $\Delta aurZ/J$. The figure is not drawn to scale. Primer sequences are listed in [supplemental Table S1](#). The size of the deletion is listed as the number of removed base pair positions when compared with the size of the coding sequence.

graminearum Genome Database (9). Multiple sequence alignments were constructed using ClustalW version 2 with default settings (12). Ad hoc *ab initio* gene modeling was performed using FGENESH and FGENESH+ (SoftBerry). Motifs in unaligned sequences were identified using MetaMEME version 4.1.1 and MAST (13, 14). Primer design and standard sequence manipulations were performed using Vector NTI 11 (Invitrogen). Identification of known motifs was performed using the Conserved Domain Database (15). SignalP 3.0 and TargetP 1.1 were used for prediction of signal peptides and subcellular localization (16, 17). TMHMM (version 2.0) was used to predict transmembrane helices (18). Predictions of glycosylphosphatidylinositol anchor locations were performed with big-PI Fungal Predictor (19). Secondary structure predictions were performed with DSSP (20) and PSIPRED (21) using PRALINE (22). HHpred 1.6.0.0 (23) was used to identify proteins that share secondary structure features similar to those predicted for AurZ, by searching the pdb70_2Oct10 database with default settings.

Targeted Gene Replacement—Binary vectors for targeted replacement of *aurT*, *aurZ*, and *aurS* were constructed by four-fragment In-Fusion cloning (Clontech) (24). The recombination flanks (geneX-A1/A2 and geneX-A3/A4) (Fig. 1) were amplified by PCR using Phusion DNA polymerase (Finnzyme) with gDNA from *F. graminearum* PH-1 as template. The pAg1-H3 vector was prepared for cloning by sequential digestion with SmaI and SwaI. The primer pairs ([supplemental Table](#)

[S1](#)) used for amplification of the inserts included 30–34-bp-long 5′-overhangs that introduced terminal extensions into the amplicons, identical to the sequences surrounding the used restriction enzyme sites in the vector. The inserts in the replacement vectors pAg1-H3: $\Delta aurT$, pAg1-H3: $\Delta aurS$, and pAg1-H3: $\Delta aurZ$ were sequenced by GATC Biotech (Constance, Germany) to verify correct insertion events. The *aurZ* (FG02325.1) and *aurJ* (FG02326.1) loci are neighbors in the aurofusarin gene cluster, separated by 319 bp, allowing replacement of both genes in a single experiment. The replacement vector was constructed using the *aurZ*-A1/A2 (this study) and the *aurJ*-A1/A2 (5) recombination flanks. The *aurZ*-A1/A2 fragment was cloned into the SmaI site of the vector by In-Fusion cloning followed by ligase-dependent cloning of the *aurJ*-A1/A2 fragment into the SpeI/SalI digested vector, as described in Ref. 5. The verified replacement vectors were transformed into *F. graminearum* PH-1 by *Agrobacterium tumefaciens*-mediated transformation as described in Refs. 4 and 5. Correct *aurT*, *aurZ*, and *aurS* replacement strains were identified by diagnostic PCR, using four primer pairs: Hyg588U/L, geneX-T1/T2, and different combination of the RF-1 and RF-2 primers with geneX-T3 and geneX-T4 primers as specified in [supplemental Table S1](#) and Fig. 1. The $\Delta aurZ/J$ strain was analyzed using: Hyg588U/L, *aurZ*-T1/T2, *aurJ*-T1/T2, *aurJ*-T1/RF1, and *aurJ*-T2/RF-2. Transformants that proved correct by the PCR analysis were verified by Southern blot analysis, using the 588-bp-long fragment of the *hph* gene as probe, amplified from

pAg1-H3 using the primers Hyg588U/L. Genomic DNA from the wild type and the different deletion strains were digested with Sall ($\Delta aurZ$:8575 bp, WT:6101 bp), NsiI ($\Delta aurT$:10915 bp, WT:4321 bp), NheI ($\Delta aurS$:9740, WT:8137 bp), and BpII ($\Delta aurZ/J$: 8787 bp, WT: 8047 bp). Southern blotting was performed as described in Ref. 5.

Initial Chemical Analysis of the Mutants—The wild type, $\Delta aurT$, $\Delta aurS$, $\Delta aurZ$, $\Delta aurZ/J$, $\Delta aurJ$, and $\Delta aurF$ strains were grown for 10 days on defined *Fusarium* medium in darkness at 25 °C (4). Metabolites were extracted using methanol:dichloromethane:ethyl acetate 1:2:3 (v/v) and, after 1% formic acid was added, analyzed by reversed-phase high-performance liquid chromatography-diode array detection (HPLC-DAD), as described in Ref. 5. To monitor aurofusarin accumulation in the $\Delta aurT$ strain as a function of time, the mutant and wild type were grown on defined *Fusarium* medium in darkness at 28 °C for 4, 5, 6, and 9 days, at which time points 4-mm diameter agar plugs were cut out, covering the area from the center to the edge of the plates. The plugs were stored at –20 °C for later analysis. Metabolites were extracted as described above, and the ergosterol content was determined by HPLC-DAD using a GROM-SIL 120 ODS-5ST, 3 μ m, 60 \times 4.6-mm inner diameter column (Grom Analytik +HPLC GmbH). Analytes were eluted with methanol with 0.1% phosphoric acid using a flow rate of 1 ml/min for 12 min as described previously (25, 26). A 100 μ g/ml ergosterol standard (Sigma-Aldrich) was used to identify and verify the ergosterol peak in the chromatograms based on retention time and UV spectrum (26). The samples were adjusted to similar ergosterol contents by dilution with methanol, and the aurofusarin and rubrofusarin contents were measured by HPLC-DAD as described in Ref. 5. The metabolite experiments were performed with at least three biological replicates.

Purification and Structural Characterization of the *aurZ*-specific Compound YWA1—The $\Delta aurZ$ mutant was grown at room temperature in darkness for 14 days on agar plates containing Bells medium (27) with maltose as the carbon source and urea as the nitrogen source as described in Ref. 4. The plates were freeze-dried, and the material (25 g) was extracted for 4 h at room temperature with 1 liter of methanol. The brown greenish extract was filtered and concentrated *in vacuo* to yield a dark brown oily residue. 100 ml of brine and ~1 liter of ethyl acetate were added to the condensed extract. The collected organic phase was dried over $MgSO_4$, filtered through a plug of Celite, and concentrated *in vacuo* to yield a black oily substance. The fungal material was extracted twice using this method to yield ~500 mg of crude extract. The crude extract was subjected to flash chromatography using a 9-g KP-SIL column (150 \times 12 mm, 40–63 μ m, 60 Å, Biotage AB, Uppsala, Sweden) and a Biotage Quad 3 Flash Collector (Biotage AB). The analytes were eluted with dichloromethane:methanol:acetic acid 95:5:0.1. Fractions were assessed for content of YWA1 by liquid chromatography-mass spectrometry (LC-MS) on a system described elsewhere (28) and by reversed-phase HPLC using a Merck-Hitachi system (Hitachi, Ltd., Tokyo, Japan) consisting of a D-7000 interface, an L-7100 pump, an L-7200 autosampler, an L-7300 column oven, and an L-7450 DAD and controlled by LaChrom analysis software. The col-

umn used was a Zorbax, Eclipse XDB-C18, 4.6- \times 75-mm inner diameter, 3.5 μ m (Rockland Technologies, Hewlett Packard) kept at 40 °C. The separations were performed at 0.5 ml/min with water:methanol:trifluoroacetic acid 90:10:0.1 (mobile phase A) and methanol:water:trifluoroacetic acid 90:10:0.1 (mobile phase B) using the following linear gradient elution profile: 0 min, 20% B; 2 min, 20% B; 12 min, 80% B; 13 min, 20% B; 15 min, 20% B. Fractions containing almost pure YWA1 were combined, whereas other fractions containing YWA1 were rechromatographed as described above but with dichloromethane:methanol:acetic acid 93:7:0.1 as eluent. YWA1-containing fractions from both separations were combined to yield 20 mg of material. The target compound was further purified by preparative scale HPLC using a Waters system described elsewhere (28). The column used was a 100 \times 19 mm-inner diameter, 5 μ m, Phenomenex Gemini C-18 (Phenomenex Inc., Torrance, CA) operated at room temperature. The separations were performed at 10 ml/min with water:trifluoroacetic acid 1000:1 (mobile phase A) and acetonitrile:trifluoroacetic acid 1000:1 (mobile phase B) using the following linear gradient elution profile: 0 min, 5% B; 2 min, 5% B; 25 min, 95% B; 27 min, 5% B; 30 min, 5% B, resulting in isolation of 9 mg of pure YWA1. High-resolution MS for exact mass determination was performed on the above instrument. NMR experiments were performed at ambient temperature on a Bruker Avance NMR spectrometer (1H frequency of 300.13 MHz) equipped with a 5-mm broad band observe probe or a Bruker Avance III NMR spectrometer (1H frequency of 799.96 MHz) equipped with a 5-mm cryogenic triple cooled inverse probe. Samples were prepared in dimethyl sulfoxide- d_6 and transferred to a 2.5-mm NMR tube.

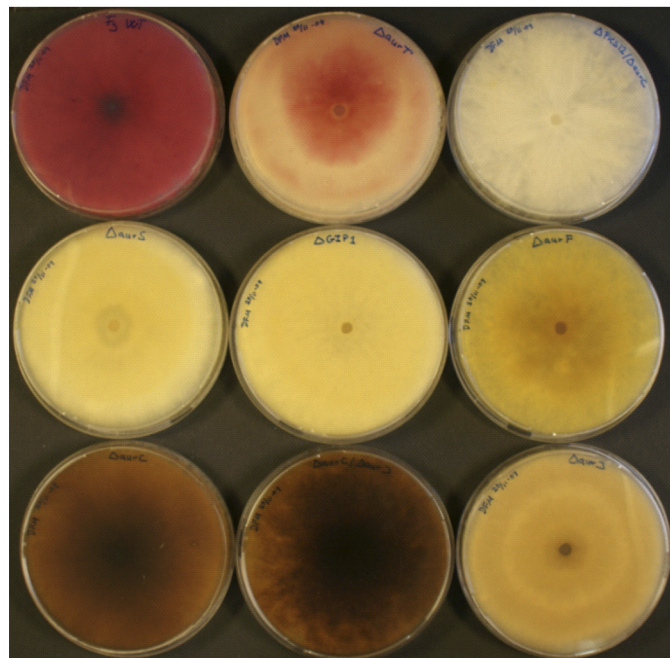
RESULTS

***aurT*, *aurZ*, and *aurS* Are All Involved in Aurofusarin Biosynthesis**—Construction of binary replacement vectors was performed by single-step four-fragment In-Fusion cloning, resulting in 10–20% correct *E. coli* transformants. *Agrobacterium tumefaciens* mediated transformation of *F. graminearum* with the constructed vectors resulted in 36 *aurZ*, 36 *aurT*, and 107 *aurS* hygromycin B-resistant transformants, with a double crossover frequency of 11, 78, and 74% based on the diagnostic PCR analysis. Five transformants for each of the deletion constructs were analyzed by Southern blot analysis, which showed that all selected transformants contained just a single tDNA copy (Fig. 2). The altered pigmentation of the verified replacement strains indicated that all three genes were involved in aurofusarin biosynthesis. The $\Delta aurZ$ strain displayed a brown/green mycelium pigmentation not observed in previous mutants (Fig. 2). The $\Delta aurS$ strain displayed a yellow pigmentation similar to that observed for the $\Delta GIP1$ and $\Delta aurF$ strains, suggesting accumulation of the intermediate rubrofusarin. The color phenotype of the $\Delta aurT$ strain was both time-dependent and temperature-dependent, but under all analyzed incubation conditions, it differed from that of the wild type. In young $\Delta aurT$ cultures, the mycelium was pink, whereas it turned red in older cultures, suggesting a delayed production of aurofusarin.

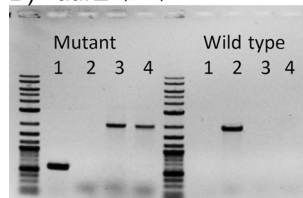
***aurZ* Homologs Are Associated with Polyketide Synthases**—The 514-bp-long *aurZ* gene (FG02325) consists of two exons,

Biosynthesis of Aurofusarin in *F. graminearum*

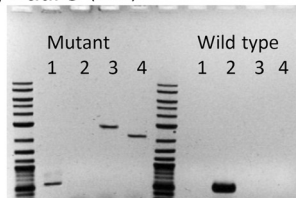
A) Phenotype of targeted deletion mutants



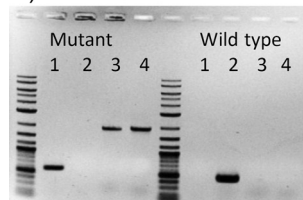
B) $\Delta aurZ$ (9-3)



C) $\Delta aurS$ (T55)



D) $\Delta aurT$ (6-1)



E) $\Delta aurZ/J$ (4-1)

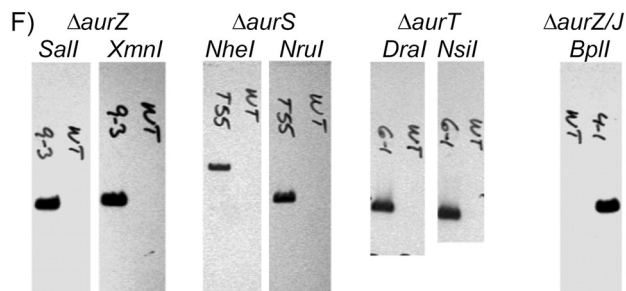
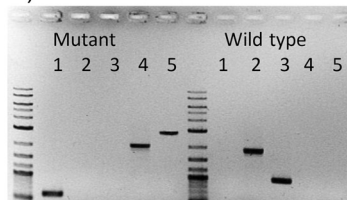


FIGURE 2. Analysis of the generated strains. A, phenotype of the constructed mutants (*) and previously constructed strains (8) grown for 10 days on defined *Fusarium* medium. Top left to right bottom, *Fg* PH-1 wild type, $\Delta aurT$ (*), $\Delta PKS12/\Delta aurZ$ (*), $\Delta aurS$ (*), $\Delta GIP1$, $\Delta aurF$, $\Delta aurZ$ (*), $\Delta aurZ/J$ (*), and $\Delta aurJ$. B–F, verification of genetically modified strains. B, PCR analysis of $\Delta aurZ$. C, PCR analysis of $\Delta aurS$. D, PCR analysis of $\Delta aurT$. E, PCR analysis of $\Delta aurZ/J$. F, Southern blot analysis of hph/tDNA copy number in the selected transformants. Lanes in B–D: lane 1 = hyg588U/L; lane 2 = check for target CDS; lane 3 = check of crossover in left flank; and lane 4 = crossover in right flank. Lanes in E: lane 1 = hph588U/L; lane 2 = *aurZ*-T1/T2; lane 3 = *aurZ*-J1/T2; and lanes 4 and 5, similar to 3 and 4 in B–D.

398 and 61 bp, separated by a 55-bp-long intron. The resulting 152-amino acid (aa) protein did not show identity to any previously characterized proteins and did not contain any described catalytic or structural domains. The available annotated fungal genome sequences were searched for AurZ homologs by position-specific iterative basic local alignment search tool (PSI-BLAST) with five recurring rounds. A total of 37 sequences with a high level of similarity were obtained from 19 ascomycetes and 2 basidiomycetes (Table 1). Analysis of the genomic regions surrounding the hits showed that 23 of the 38 AurZ homologs were located less than 10 genes away from PKS-encoding genes. 17 of the 23 PKS genes encoded non-reducing polyketide synthases similar to PKS12 in the aurofusarin gene cluster.

A multiple sequence alignment of the 20 proteins that showed the highest level of similarity to AurZ revealed that the sequences shared 8 fully conserved sequence positions and 33 positions with similar properties (supplemental Fig. S1). The search for conserved sequence motifs, using Meta-MEME, revealed four conserved domains with high information content and a total of 24 highly or fully conserved sequence positions (supplemental Fig. S2). The analyzed sequences were predicted to have very similar secondary structures including four helices and four strands, as seen by multiple alignment based on secondary structure (supplemental Fig. S3).

The search for structurally related proteins based on similarities in secondary structure resulted in over 50 high scoring hits in the Protein Data Bank (PDB) covering the entire primary sequence of AurZ (Table 2). The proteins all displayed very limited identity on the primary sequence level but a highly similar tertiary structure belonging to the split α - β sandwich group (ferredoxin-like fold) of the $\alpha + \beta$ fold class of proteins. Alignment guided by the secondary structure of AurZ and enzymes, for which biochemical data were available, showed that the enzymes did not share any conserved residues in the known active sites of the characterized enzymes (supplemental Fig. S3).

The reversed-phase HPLC-DAD analysis of the targeted *aurZ* deletion mutant showed that it accumulated a new compound (retention time 3.23 min) not found in the wild type or any of the previously described aurofusarin-deficient mutants (Fig. 3C). The UV-visible spectrum for the compound displayed a high level of similarity to that of rubrofusarin and nor-rubrofusarin, suggesting that the compounds were structurally related with respect to their conjugated ring systems (Fig. 3, J–L). The metabolite eluted ~45 s prior to nor-rubrofusarin and 170 s prior to rubrofusarin, showing that the compound was more hydrophilic than any of the known intermediates in the aurofusarin pathway. High-resolution-MS analysis showed that it had an m/z of 277.0712 (= $[M+H]^+$) and 259.0617 (= $[M+H-H_2O]^+$), equivalent to a molecular formula of $C_{14}H_{12}O_6$, which implies that the compound had two more hydrogen and one more oxygen atom than nor-rubrofusarin. The similarity of the new $\Delta aurZ$ metabolite to an *Aspergillus* spore pigment (29) with respect to 1H NMR (supplemental Table S2) and UV-spectral data established its identity as YWA1. The presence of an additional hydroxyl group in YWA1 when compared with nor-rubrofusarin coincides with a shorter retention time as observed for the new metabolite. Equilibrium

TABLE 1

Identified AurZ homologs and their relative position to the nearest PKS encoding gene

Listed after succeeding identity (I) to AurZ, similarity (S), and length (L). Not found (-).

Hit	AurZ homologs			Closest PKS encoding gene on genome		
	Species	Accession No.	I/S/L	Distance	Accession No.	PKS domains
0	<i>Fusarium graminearum</i>	FG02325.1	-/-/152	+ 1 (0.5 kb)	FG12040	KS-AT-ACP-CYC
1	<i>Talaromyces stipitatus</i>	TSTA_058090	69/53/183	+ 2 (1.5 kb)	TSTA_058110	AMP dependent CoA ligase
2	<i>Pyrenophora tritici-repentis</i>	PTRG_02729	69/48/186	-	-	-
3	<i>Microsporium canis</i>	MCYG_05053	68/50/137	+ 1 (0.3 kb)	MCYG_05054.1	KS-AT-ACP-ACP-CYC
4	<i>Neosartorya fischeri</i>	NFIA_101890	67/51/146	+ 7 (12 kb)	NFIA_101810	KS-AT-ACP
5	<i>Talaromyces stipitatus</i>	TSTA_126440	66/57/152	-	-	-
6	<i>Penicillium marneffeii</i>	PMAA_100350	66/56/187	+ 1 (0.2 kb)	PMAA_100360	KS-AT-ACP
7	<i>Aspergillus fumigatus</i>	Afu4g14470	66/51/142	+ 9 (12 kb)	Afu4g14560	KS-AT-ACP
8	<i>Penicillium marneffeii</i>	PMAA_031690	65/55/180	+ 5 (11 kb)	PMAA_031640	KS-AT-ACP
9	<i>Microsporium canis</i>	MCYG_06698	65/51/188	+ 8 (12 kb)	MCYG_06706	KS
10	<i>Neosartorya fischeri</i>	NFIA_101630	63/57/151	+ 3 (2.5 kb)	NFIA_101660	KS-AT-ACP
11	<i>Aspergillus terreus</i>	ATEG_08457	62/47/142	+ 6 (8 kb)	ATEG_08451	KS-AT-ACP
12	<i>Aspergillus nidulans</i>	ANID_11847.1	60/55/139	+ 1 (0.3 kb)	ANID_00150.1	KS-AT-ACP
13	<i>Talaromyces stipitatus</i>	TSTA_008960	60/54/167	+ 1 (1 kb)	TSTA_008950	KS-AT-ACP-CYC
14	<i>Aspergillus oryzae</i>	AO090001000323	59/50/137	-	-	-
15	<i>Aspergillus flavus</i>	AFL2G_07546	59/50/137	-	-	-
16	<i>Chaetomium globosum</i>	CHGG_08978	56/50/147	-	-	-
17	<i>Penicillium chrysogenum</i>	Pc16g10800	55/53/143	+ 5 (?)	Pc16g10750	KS-AT-ACP
18	<i>Aspergillus niger</i>	e_gw1_14.245	54/56/133	+ 1 (0.8 kb)	e_gw1_14.257	KS-AT-ACP-ACP-CYC
19	<i>Talaromyces stipitatus</i>	TSTA_083280	51/55/133	+ 3 (3.7 kb)	TSTA_083310	KS-AT-ACP-CYC
20	<i>Penicillium marneffeii</i>	PMAA_063590	49/55/130	+ 3 (4.1 kb)	PMAA_063620	KS-AT-ACP-CYC
21	<i>Phaeosphaeria nodorum</i>	SNOG_08275	46/54/127	+ 1 (1.8 kb)	SNOG_08274	KS-AT-ACP-CYC
22	<i>Aspergillus nidulans</i>	AN1088.2	45/50/127	-	-	-
23	<i>Penicillium marneffeii</i>	PMAA_043660	39/53/139	-	-	-
24	<i>Aspergillus niger</i>	An11g06450	38/50/165	+ 1 (1 kb)	An11g06460	KS-AT-DH-KR-ACP
25	<i>Magnaporthe grisea</i>	MGG_14687.6	37/61/126	+ 4 (7.8 kb)	MGG_00428.6	KS-AT-ACP-CYC
26	<i>Pyrenophora tritici-repentis</i>	PTRG_10876	36/57/144	-	-	-
27	<i>Aspergillus niger</i>	An02g08300	36/54/164	+ 1 (0.8 kb)	An02g08290	KS-AT-DH-KR
28	<i>Fusarium graminearum</i>	FGSG_13420.3 ^a	35/65/183	+ 8 (35 kb)	FGSG_08208.3	KS-AT-DH-ER-KR-ACP
29	<i>Fusarium oxysporum</i>	FOXG_16598.2	35/63/180	+ 29 (71 kb)	FOXG_16568.2	AMP dependent CoA ligase
30	<i>Monilophthora perniciosa</i>	MPER_10734	35/56/200	-	-	-
31	<i>Nectria haematococca</i>	EEU41176.1	35/51/161	-	-	-
32	<i>Ustilago maydis</i>	UM05965.1	34/65/153	-	-	-
33	<i>Talaromyces stipitatus</i>	TSTA_000620	34/54/131	-	-	-
34	<i>Fusarium graminearum</i>	FGSG_03463.3	33/53/177	-	-	-
35	<i>Fusarium verticillioides</i>	FVEG_01729.3	29/71/184	+ 6 (14 kb)	FVEG_01736.3	KS-AT-DH-ER-KR-(no ACP)
36	<i>Fusarium oxysporum</i>	FOXG_02891	29/69/184	+ 7 (10 kb)	FOXG_02884.2	KS-AT-DH-KR
37	<i>Fusarium verticillioides</i>	FVEG_13655.3	29/54/147	+ 14 (45 kb)	FVEG_13670.3	AMP dependent CoA ligase

^a Modified gene models.

TABLE 2

Top 20 proteins and proteins with known function displaying similar secondary structure as predicted for AurZ

SS = secondary structure score for how well the PSIPRED-predicted (three-state) or actual DSSP-determined (eight-state) secondary structure sequence agree with each other. I = identity on primary sequence level for aligned region.

Hit	PDB identifier	Predicted function (origin)	SS	Coverage	I
1	3HF5_A; 3HDS_A; 3HFK_A; 2IFX_A (MLMI)	4-Methylmuconolactone methylisomerase (<i>Pseudomonas reinekei</i>)	11.0	108 aa	15%
2	2FTR_A	Unknown (<i>Bacillus halodurans</i>)	11.9	106 aa	14%
3	3BF4_A	Ethyl TERT-butyl ether degradation (<i>Ralstonia eutropha</i>)	11.5	103 aa	10%
4	1TR0_A; 1SI9_A	Stress protein (unknown function) (<i>Populus tremula</i>)	13.7	106 aa	10%
5	2JDJ_A (HapK)	Prodigiosin biosynthesis (unknown) (<i>Hahella chejuensis</i>)	10.2	82 aa	11%
6	3BB5_A	Stress responsive alpha-beta protein (<i>Jannaschia sp</i>)	12.6	103 aa	10%
7	2FB0_A	Unknown (<i>Bacteroides thetaiotaomicron</i>)	10.5	78 aa	8%
8	1Q4R_A; 1Q53_A; 2Q3P_A	Unknown (<i>Arabidopsis thaliana</i>)	11.6	106 aa	15%
9	2OMO_A	Predicted oxidoreductase (<i>Nitrosomonas europaea</i>)	11.0	121 aa	14%
10	3FMB_A	Unknown (<i>Bacteroides fragilis</i>)	13.3	101 aa	13%
11	2GYC_A	Unknown (<i>Bordetella bronchiseptica</i>)	12.7	96 aa	10%
12	3BDE_A	Unknown (<i>Mesorhizobium loti</i>)	12.0	97 aa	18%
13	3LO3_A	Unknown (<i>Colwellia psychrerythraea</i>)	8.2	66 aa	8%
14	3E80_A	Unknown (<i>Deinococcus radiodurans</i>)	11.6	105 aa	11%
15	3BN7_A	Unknown (<i>Caulobacter crescentus</i>)	12.0	86 aa	14%
16	3KG0_A; 3KG1_A; 3KNG_A (SnoB)	Anthracycline monooxygenase (<i>Streptomyces nogalater</i>)	9.7	98 aa	18%
17	1IUJ_A (TT1380)	Unknown (<i>Thermus thermophilus</i>)	9.5	100 aa	13%
18	1X7V_A (PA3566)	Unknown (<i>Pseudomonas aeruginosa</i>)	11.3	82 aa	13%
19	1Q8B_A	Unknown (<i>Bacillus subtilis</i>)	9.1	95 aa	7%
20	3BM7_A	Unknown (<i>Caulobacter crescentus</i>)	10.0	79 aa	14%
28	1TUV_A; 1R6Y_A (YgiN)	Menadione oxidase (<i>Escherichia coli</i>)	11.8	86 aa	10%
35	1SQE_A; 2ZDP_A; 3LGM_A; 3LGN_A (IsdG/I)	Heme-degrading enzyme (<i>Staphylococcus aureus</i>)	6.3	75 aa	11%
37	1Y0H_A	Monooxygenase (<i>Mycobacterium tuberculosis</i>)	7.8	102 aa	9%

between YWA1 and the ring-opened diketo tautomer was observed when YWA1 was dissolved in dipolar aprotic solvents such as dimethyl sulfoxide. The ¹H NMR resonances of the ring-opened form of YWA1 (supplemental Table S2) are com-

parable with those found for the related structure 2-acetyl-1,3,6,8-tetrahydroxynaphthalene (30), except for H-10, whose resonance frequency will be affected by the hydrogen-bonding scheme for its neighboring OH group.

Biosynthesis of Aurofusarin in *F. graminearum*

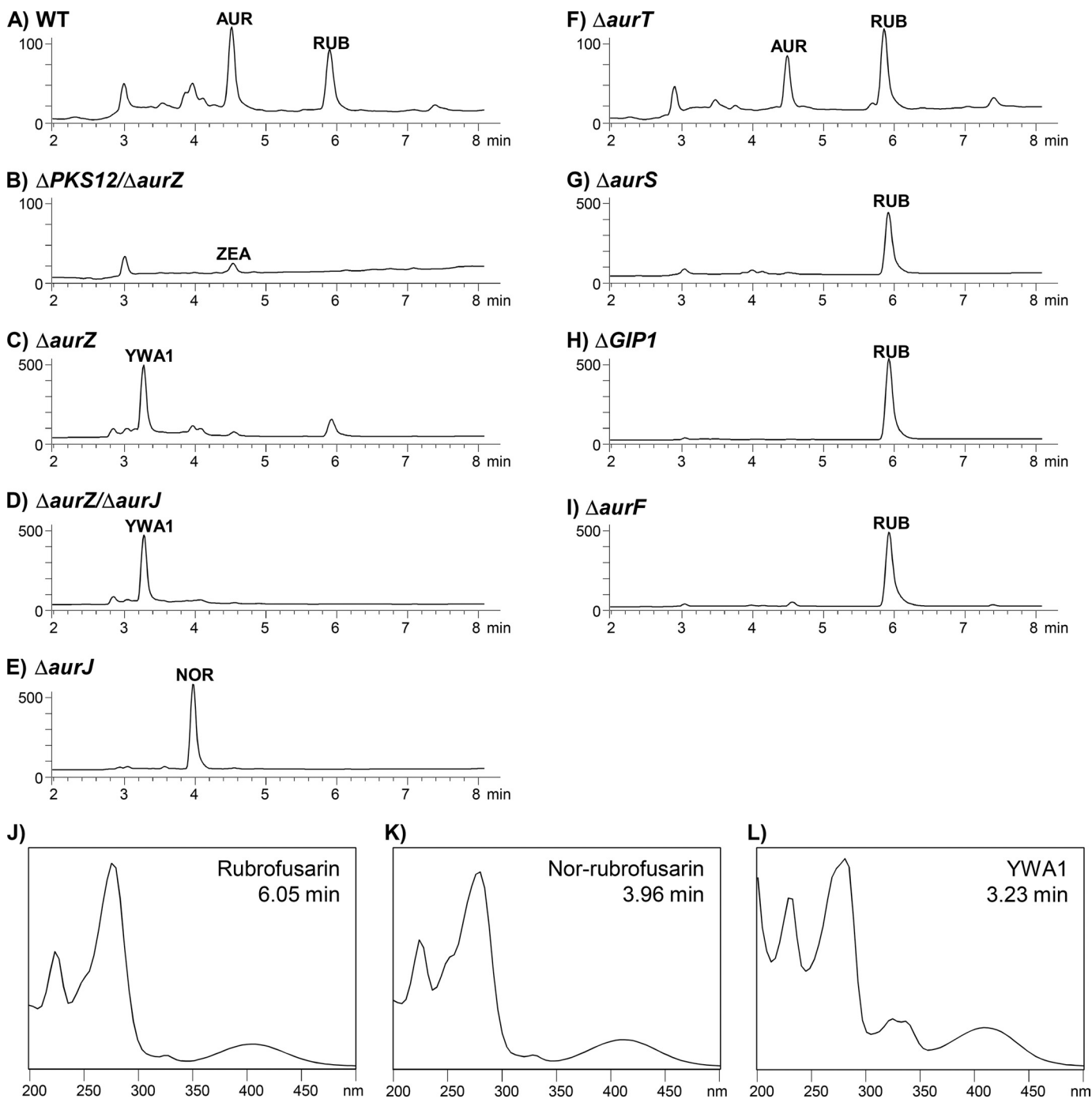


FIGURE 3. Reversed-phase HPLC-DAD analysis of genetically modified *F. graminearum* strains. A–I, chromatograms showing UV absorption (milliabsorbance units, 230 nm) as a function of retention time (min). A, wild type. AUR, aurofusarin; RUB, rubrofusarin. B, $\Delta aurPKS12/aurZ$. ZEA, zearalenone. C, $\Delta aurZ$. D, $\Delta aurZ/J$. E, $\Delta aurJ$. NOR, nor-rubrofusarin. F, $\Delta aurT$. G, $\Delta aurS$. H, $\Delta GIP1$. I, $\Delta aurF$. J–L, UV-visible absorption spectra. J, rubrofusarin. K, nor-rubrofusarin. L, YWA1. Note the different y axes in the chromatograms.

AurZ Acts as the First Tailoring Enzyme in the Aurofusarin Biosynthetic Pathway—Simultaneous replacement of *aurZ* and *aurJ* resulted in 24 transformants with a double crossover frequency of 62.5%. The double replacement strain $\Delta aurZ/J$ accumulated YWA1, like the $\Delta aurZ$ strain, and not nor-rubrofusarin, as found in the $\Delta aurJ$ strain, showing that AurZ functions prior to AurJ during aurofusarin biosynthesis (Fig. 3, C–E). This finding suggests that the primary product of PKS12 is YWA1 and not nor-rubrofusarin as reported previously (5).

Targeted replacement of *aurZ* resulted in three different color phenotypes: red, yellow/green, and white mycelium. The PCR-based analysis showed that red transformants represented single crossover events where *aurZ* had not been replaced, and the yellow/green and white transformants were true *aurZ* replacements lacking the *aurZ* gene. Sequencing of the upstream recombination flank that extends into the *PKS12* locus revealed that a single-nucleotide substitution of guanine (G) to thymine (T) had

TABLE 3
Identified AurS homologs

I = identity, S = similarity and E = expected value. The locations of the two fasciclin domains are shown in the right hand column.

Hit	Species	Accession no.	I	S	E	Fasciclin domains
1	<i>Microsporium canis</i>	MCYG_08538	160/404	235/404	6e-72	93–193; 207–352
2	<i>Ajellomyces capsulatus</i>	HCAG_03186	107/359	171/359	2e-36	142–256; 271–414
3	<i>Sclerotinia sclerotiorum</i>	SS1G_05049	126/377	186/377	6e-36	156–278; 296–451
4	<i>Ajellomyces capsulatus</i>	HCBG_05627	108/358	174/358	8e-36	158–260; 274–417
5	<i>Ajellomyces dermatitidis</i>	BDCG_02276	106/334	157/334	1e-34	166–269; 283–426
6	<i>Ajellomyces dermatitidis</i>	BDBG_06929	106/334	157/334	1e-34	166–269; 282–426
7	<i>Ajellomyces capsulatus</i>	HCDG_08956	102/326	158/326	4e-34	158–260; 274–417
8	<i>Botryotinia fuckeliana</i>	BC1G_09860	115/367	179/367	2e-32	155–279; 297–452
9	<i>Coccidioides posadasii</i>	CPC735_024720A	109/370	172/370	3e-32	121–247; 271–403
10	<i>Coccidioides immitis</i>	CIMG_05852	108/370	171/370	1e-31	124–247; 271–403
11	<i>Aspergillus terreus</i>	ATEG_00632	109/381	184/381	2e-31	133–264; 278–429
12	<i>Penicillium marneffeii</i>	PMAA_005700	109/368	174/368	4e-31	226–328; 342–488
13	<i>Uncinocarpus reesii</i>	UREG_04495	107/356	167/356	6e-31	129–255; 270–412
14	<i>Pyrenophora tritici-repentis</i>	PTRG_06147	106/369	174/369	8e-30	162–288; 302–451
15	<i>Phaeosphaeria nodorum</i>	SNOG_07701	103/361	173/361	1e-29	141–267; 281–431
16	<i>Aspergillus fumigatus</i>	AFUB_013850A	107/375	169/375	3e-27	142–279; 298–446
17	<i>Aspergillus clavatus</i>	ACLA_021110	109/383	171/383	5e-27	145–289; 337–456
18	<i>Talaromyces stipitatus</i>	TSTA_104300	104/364	176/364	8e-27	200–330; 344–493
19	<i>Aspergillus fumigatus</i>	AfA10A1.015	103/377	168/377	1e-26	142–279; 298–446
20	<i>Neosartorya fischeri</i>	NFIA_011110	105/371	168/371	2e-26	142–282; 297–444
21	<i>Nectria haematococca</i>	NECHADRAFT_92290	100/369	177/369	2e-26	100–228; 242–389
22	<i>Aspergillus flavus</i>	AFLA_042090	108/378	172/378	5e-24	132–260; 275–421
23	<i>Penicillium chrysogenum</i>	Pc16g12870	100/352	161/352	6e-24	282–386; 399–561
24	<i>Aspergillus oryzae</i>	AO090011000381	104/350	160/350	2e-23	132–260; 275–421
25	<i>Aspergillus nidulans</i>	AN0768.2	104/391	170/391	2e-23	131–278; 300–447
26	<i>Gibberella zeae</i>	FG02859	103/380	174/380	7e-23	114–241; 255–397
27	<i>Podospora anserina</i>	PODANSg4381	99/343	154/343	8e-23	115–245; 260–404
28	<i>Aspergillus niger</i>	An15g02640	96/366	154/366	2e-19	57–179; 196–366

occurred in the white mutants. The substitution was located inside the predicted malonyltransferase (MAT) domain of PKS12 (693G→T), changing Ala¹⁹³ to Val¹⁹³ and most likely rendering the resulting enzyme dysfunctional. The lack of YWA1 accumulation in the resulting Δ PKS12/ Δ aurZ strain shows that PKS12 synthesizes the compound that accumulates in the Δ aurZ strain. The base substitution was located in the terminal part of the replacement tDNA, allowing for the generation of both correct Δ aurZ mutants, by crossover close to the hygromycin resistance gene in the tDNA, and double mutants, by crossover close to the terminal end of the recombination flank in the tDNA.

aurS Mutants Accumulate Rubrofusarin—The 1281-bp-long *aurS* gene consists of two exons separated by a 48-bp intron and encodes a 407-aa-long protein. AurS did not show homology to any previously characterized proteins in GenBank; however, the search for conserved domains revealed two fasciclin domains (COG2335) at positions 52–192 and 195–365.

30 sequences displaying a high level of identity to AurS were identified by blastp, all of which contained two fasciclin domains (Table 3). Multiple sequence alignment revealed that the identified sequences shared 27 fully conserved positions and 117 positions with similar properties (supplemental Fig. S4). The search for conserved sequence motifs in the unaligned sequences (Meta-MEME analysis) showed that the proteins varied considerably in the N-terminal region with respect to both sequence and length but that they shared similar motifs and motif architecture in the C-terminal end (~350 aa). The conserved C-terminal region was described by eight motifs covering 248 amino acid positions, including 82 highly or fully conserved positions (supplemental Fig. S5). The novel conserved motifs that were identified by this Meta-MEME analysis are shown in supplemental Fig. S6. Analysis of the genomic region

adjacent to the identified AurS homologs showed that they did not co-localize with PKS or non-ribosomal peptide synthetase encoding genes.

The MIPS annotation of AurS includes the prediction of a transmembrane domain located from positions 7 to 29, and an analysis using SignalP suggests that this N-terminal sequence contains a signal peptide, which is cleaved between Ser³⁶ and Gln³⁷. This combined with a TargetP prediction suggests that the signal peptide induces secretion of the protein to the extracellular surface of the cell (score: 0.899). Fungal fasciclin-like proteins have been reported to be tethered to the outer leaflet of the plasma membrane by glycosylphosphatidylinositol anchors (31), but a search for glycosylphosphatidylinositol anchor sites in AurS and homologs did not find any sites with a significant score. Prediction of subcellular localization for the identified homologs showed that 28 of the 30 analyzed sequences are probably excreted. Targeted replacement of *aurS* resulted in an aurofusarin-deficient strain that accumulated rubrofusarin (Fig. 3G), which previously has been demonstrated to accumulate in Δ GIPI, Δ aurO, and Δ aurF strains (Fig. 3, H and I) (5).

AurT Encodes a Major Facilitator-type Efflux Pump—The *aurT* (FG02322) gene consists of two exons, 629 and 1006 bp, separated by a 63-bp-long intron, resulting in a total coding sequence of 1635 bp, equivalent to a protein of 544 amino acids. The deduced amino acid sequence shows significant similarity to major facilitator-type efflux pumps. The highest similarity was found to the hypothetical protein nh_02161 from *Nectria haematococca* mpVI (identity = 55.6%), and among the characterized proteins, the highest similarity was found to the sterigmatocystin (aflatoxin) efflux pump AflT from *Aspergillus nidulans* (I = 42%). The AurT sequence included 14 predicted transmembrane domains, and the N-terminal secretion signal is predicted to target the protein to the plasma or endoplasmic

Biosynthesis of Aurofusarin in *F. graminearum*

reticulum membrane. Targeted replacement of *aurT* resulted in a reduction in aurofusarin production and a doubling of the rubrofusarin-to-aurofusarin ratio when compared with that observed in the wild type (Fig. 4). Aurofusarin was continuously being synthesized, but at a lower rate than in the wild type (Fig. 3F).

DISCUSSION

Fungal secondary metabolite gene organization facilitates the characterization of the respective pathways by stepwise dissection. However, a full understanding of the pathways is still challenging, particularly when novel hypothetical proteins are involved. The detailed knowledge of the aurofusarin pathway was exploited to address the function of two novel classes of proteins. This provides important new biological insight and knowledge of the molecular machinery required for the biosynthesis of a fungal pigment.

AurZ Is Required for Dehydration of YWA1 to Nor-rubrofusarin—In previous models for aurofusarin biosynthesis, FgPKS12 was predicted to form the naphthopyrone, nor-rubrofusarin (4, 5). Here we show that *AurZ* is required for nor-rubrofusarin biosynthesis, which implies that FgPKS12 synthesizes a precursor to nor-rubrofusarin, YWA1. This is consistent with results reported for the closely related wA PKS from *A. nidulans* (32). Accordingly, the new model for aurofusarin biosynthesis includes YWA1 as the first stable intermediate in the pathway (Fig. 5A). The C2 hydroxyl group in the pyrone ring of YWA1 is probably formed during ring closure by an aldol-type cyclization reaction as described for wA in *A. nidulans* (33). The accumulation of YWA1 in the $\Delta aurZ$ strain suggests that *AurZ* is responsible for catalyzing the dehydration reaction that converts the novel intermediate into nor-rubrofusarin (Fig. 5A). As *AurZ* does not show significant sequence similarity to any previously characterized enzymes, including

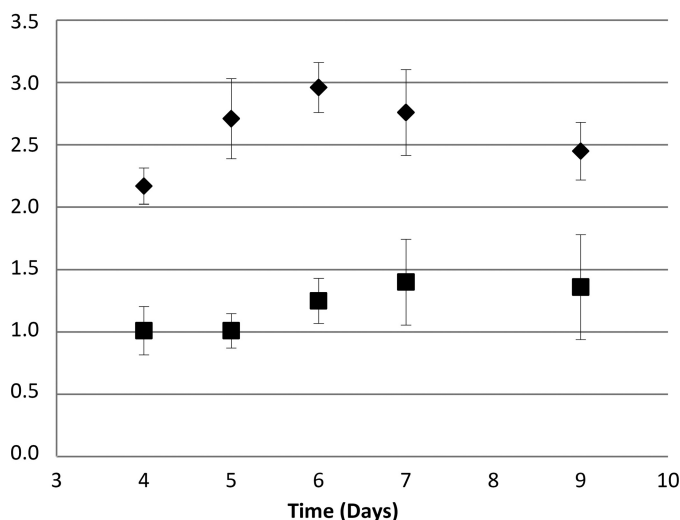


FIGURE 4. **Rubrofusarin-to-aurofusarin ratio.** A plot of the rubrofusarin-to-aurofusarin ratio in the wild type (squares) and $\Delta aurT$ (diamonds) strains is shown (each point is supported by three biological replicates). Error bars indicate S.E.

dehydratases, it is the first identified member of a novel family of dehydratases. However, further experimental data are required to establish whether the enzyme is capable of performing the dehydration by itself or whether it is dependent on additional co-factors.

The 1,8-dihydroxynaphthalene melanin pathway found in *Wangiella dermatitidis*, *Sordaria macrospora*, *Colletotrichum lagenarium*, *Magnaporthe grisea*, *Neurospora crassa*, *Alternaria alternata*, and several *Aspergillus* species is currently the best described fungal mycelium pigment biosynthetic pathway (34, 35). The pathway includes two dehydration reactions catalyzed by scytalone dehydratase (SD) (EC 4.2.1.94) (Fig. 5B) (36). The ligand-binding pocket of the enzyme is a cone-shaped

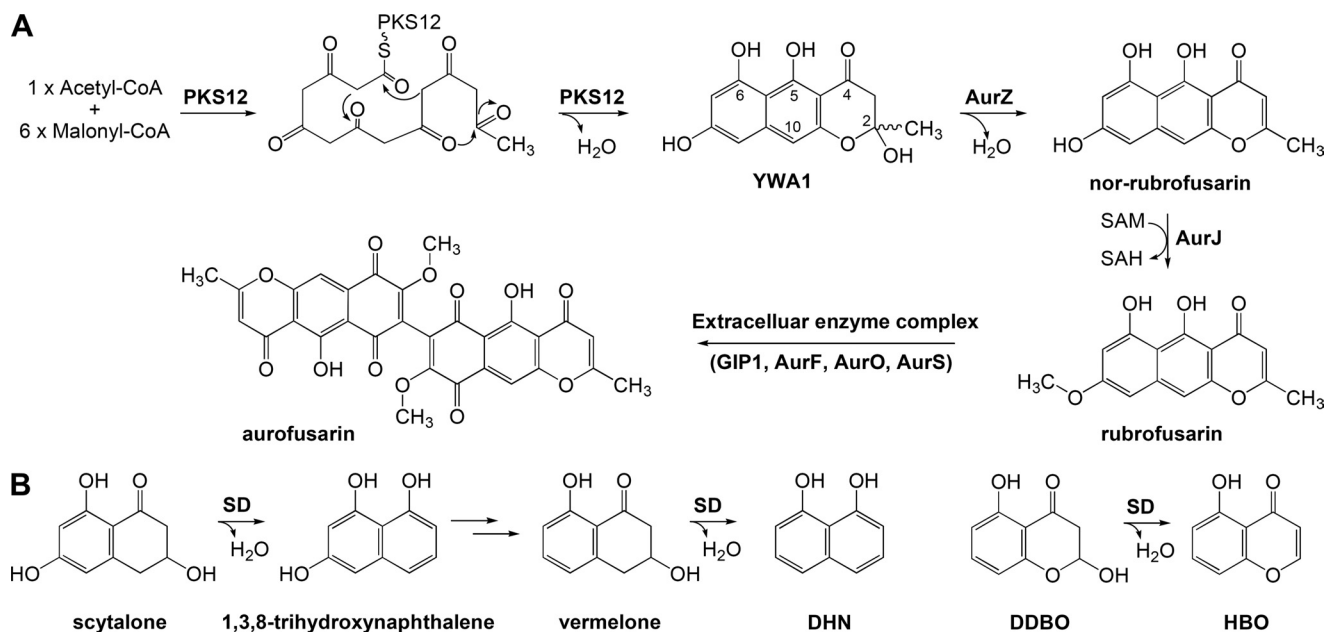


FIGURE 5. **Action of the dehydratase AurZ.** A, a revised model for the initial step of aurofusarin biosynthesis, including the suggested dehydration reaction of YWA1 catalyzed by *AurZ*. B, the action of SD in 1,8-dihydroxynaphthalene (*DHN*) melanin biosynthesis and with an alternative naphthopyrone substrate. S-adenosylmethionine (SAM), S-adenosyl-homocysteine (SAH), 2,3-dihydro-2,5-dihydroxy-4H-benzopyran-4-one (DDBO), 5-hydroxy-4H-1-benzopyran-4-one (HBO).

$\alpha + \beta$ barrel, consisting of eight β strands and four α helices sandwiched together. The enzyme acts independently of co-factors, prosthetic groups, or metal ions (37). In addition to its natural substrates, scytalone and vermelone, SD is also able to act on the pyrone 2,3-dihydro-2,5-dihydroxy-4H-benzopyran-4-one (DDBO), which resembles the structure of YWA1 (38). Although both SD and AurZ catalyze dehydration reactions of related polycyclic substrates, they have limited primary sequence identity (13% when compared with SD from *M. grisea*) but a high level of similarity in the predicted secondary structure, suggesting a similar tertiary structure (47% when compared with SD from *M. grisea*). Comparison of the characterized active site residues of SD (Tyr³⁰, Tyr⁵⁰, His⁸⁵, and His¹¹⁰) and AurZ, by secondary structure alignment, showed that these residues were not conserved in AurZ. This suggests that AurZ and SD have different catalytic mechanisms. The predicted secondary structure of AurZ and the homologs listed in Table 1 displayed a high level of similarity to several proteins that have been structurally characterized (Table 2). Common to these proteins is a ferredoxin-like fold, consisting of a β - α - β - α - β motif with the antiparallel β strands forming the floor of the active site and the three α helices arching the β sheet structure creating a reactive cavity. This group of structurally related proteins includes enzymes responsible for 4-methylmuconolactone methyl degradation (isomerase, *Pseudomonas reinekei*) (39), ethyl *tert*-butyl ether degradation (*Ralstonia eutropha*) (PDB id 3BF4), polyketide biosynthesis (anthracycline monooxygenase, *Streptomyces nogalater*) (40), redox cycling (menadione oxidase, *Escherichia coli*) (41), and heme degradation (*Staphylococcus aureus*) (42). Although the enzymes share structural features, they catalyze very diverse types of reactions and display different active site residues. They all act independently of co-factors, prosthetic group and metals. The substrates vary greatly in size, which is reflected in the size of the active site cavities of the enzymes (43). The fact that substrates such as heme groups (porphyrin structure), anthracycline (four aromatic rings), and actinorhodin (three aromatic rings) can be accommodated by this type of protein fold makes it likely that AurZ can bind YWA1 in a similar fashion.

The double targeted replacement strains $\Delta aurZ/J$ and *PKS12/aurZ* support the proposed order of reactions in the revised model for aurofusarin biosynthesis (Fig. 5A) as the *PKS12* mutation was epistatic to the *aurZ* mutation, which in turn was epistatic to the *aurJ* mutation (Figs. 2 and 4). The close genetic linkage between AurZ homologs and non-reducing PKS genes in different fungal genomes suggests that this novel class of dehydratases is an essential part of other polyketide biosynthetic pathways that lead to the formation of aromatic compounds in fungi.

What Function Does AurS Have in the Biosynthesis of Aurofusarin?—AurS does not show homology to any previously characterized proteins but does contain two fasciclin domains. Enzymes containing fasciclin domains have been described from a wide range of eukaryotic organisms and have typically been shown to facilitate cell-cell adhesion via protein-protein interactions (44–47). This domain type was initially identified as a crucial cell adhesion protein in the nervous system of *Drosophila*. In the fungi *Lentinula edodes* and *Magna-*

porthe oryzae, they were shown to be required for morphogenesis and tissue differentiation (48, 49). However, apart from the presence of fasciclin domains, these two proteins do not show homology to AurS. The search for AurS homologs identified AfA10A1.015 (Afu4g14470) from *Aspergillus fumigatus* as a homolog (Table 3), a protein that previously has been suggested to mediate host-pathogen interaction (50). Our results are the first to indicate that proteins with fasciclin domains play a role in pigment biosynthesis.

Resolution of the steps leading to formation of rubrofusarin has been possible due to the accumulation of unique pathway intermediates after replacement of individual gene cluster members. Mutations in later steps of the pathway have all resulted in the accumulation of rubrofusarin and a lack of aurofusarin. These results are best explained by the existence of a protein complex that becomes inactive or disintegrates if any of its members are missing (5). Based on the accumulation of rubrofusarin in deletion mutants, the aurofusarin biosynthetic protein complex is predicted to include AurO, AurF, Gip1, and AurS. Three of these four proteins contain N-terminal signal peptides for export to the plasma membrane via the endoplasmic reticulum. We propose that this extracellular protein complex is responsible for converting rubrofusarin to aurofusarin (Fig. 5A).

There is evidence to suggest that many secondary metabolite biosynthetic pathways in fungi are restricted to specific organelles, as shown for cyclosporine, penicillin, and aflatoxin biosynthesis (51–56). Recently specific synthesis vesicles, aflatoxinsomes (57), were discovered in *Aspergillus parasiticus*. In the case of aurofusarin biosynthesis, the members of the putative enzyme complex all lack known retention signals, which suggests that part of this pathway is completed outside the cell.

We have recently shown that the conversion of rubrofusarin to aurofusarin is dependent on the generic trans-plasma membrane redox system (58), which suggests that conversion of rubrofusarin to aurofusarin is catalyzed outside the cell in relation to the surface of the plasma membrane. The indication that AurT is a rubrofusarin-specific pump further supports that rubrofusarin is transported across the plasma membrane for enzymatic processing. Previous reports did not detect any effect of deleting *aurT* (11), but this could be explained by the non-specific action of one or more of the 307 putative major facilitator superfamily efflux pumps present in the *F. graminearum* genome or differences in the culture conditions used.

In conclusion, our results suggest that the hypothetical protein AurZ is the first member of a previously unknown class of dehydratases acting on hydroxylated naphthopyrone ring structures. AurS is the first fasciclin domain-containing protein to be associated with fungal pigment biosynthesis. AurT is predicted to facilitate the transfer of rubrofusarin to the plasma membrane surface for conversion into aurofusarin. The results have led to a revised model for aurofusarin biosynthesis in which an additional step is included.

REFERENCES

1. Lysøe, E., Klemsdal, S. S., Bone, K. R., Frandsen, R. J., Johansen, T., Thrane, U., and Giese, H. (2006) *Appl. Environ. Microbiol.* **72**, 3924–3932
2. Varga, J., Kocsubé, S., Tóth, B., and Mesterházy, A. (2005) *Acta. Biol. Hung.* **56**, 375–388

Biosynthesis of Au-rofusarin in *F. graminearum*

- Tobiasen, C., Aahman, J., Ravnholt, K. S., Bjerrum, M. J., Grell, M. N., and Giese, H. (2007) *Curr. Genet.* **51**, 43–58
- Malz, S., Grell, M. N., Thrane, C., Maier, F. J., Rosager, P., Felk, A., Albertsen, K. S., Salomon, S., Bohn, L., Schäfer, W., and Giese, H. (2005) *Fungal Genet. Biol.* **42**, 420–433
- Frandsen, R. J., Nielsen, N. J., Maolanon, N., Sørensen, J. C., Olsson, S., Nielsen, J., and Giese, H. (2006) *Mol. Microbiol.* **61**, 1069–1080
- Kim, Y. T., Lee, Y. R., Jin, J., Han, K. H., Kim, H., Kim, J. C., Lee, T., Yun, S. H., and Lee, Y. W. (2005) *Mol. Microbiol.* **58**, 1102–1113
- Song, Z., Cox, R. J., Lazarus, C. M., and Simpson, T. J. (2004) *ChemBioChem* **5**, 1196–1203
- Gaffoor, I., Brown, D. W., Plattner, R., Proctor, R. H., Qi, W., and Trail, F. (2005) *Eukaryotic Cell* **4**, 1926–1933
- Güldener, U., Mannhaupt, G., Münsterkötter, M., Haase, D., Oesterheld, M., Stümpflen, V., Mewes, H. W., and Adam, G. (2006) *Nucleic Acids Res.* **34**, D456–D458
- Kim, J. E., Han, K. H., Jin, J., Kim, H., Kim, J. C., Yun, S. H., and Lee, Y. W. (2005) *Appl. Environ. Microbiol.* **71**, 1701–1708
- Kim, J. E., Kim, J. C., Jin, J. M., Yun, S. H., and Lee, Y. W. (2008) *Plant Pathol. J.* **24**, 8–16
- Larkin, M. A., Blackshields, G., Brown, N. P., Chenna, R., McGettigan, P. A., McWilliam, H., Valentin, F., Wallace, I. M., Wilm, A., Lopez, R., Thompson, J. D., Gibson, T. J., and Higgins, D. G. (2007) *Bioinformatics* **23**, 2947–2948
- Bailey, T. L., and Elkan, C. (1994) in *Proceedings of the Second International Conference on Intelligent Systems for Molecular Biology* (Altman, R., Brutlag, D., Karp, P., Lathrop, R., and Searls, D., eds) p. 36, The AAAI Press, Menlo Park, CA
- Bailey, T. L., and Gribskov, M. (1998) *Bioinformatics* **14**, 48–54
- Marchler-Bauer, A., Anderson, J. B., Derbyshire, M. K., DeWeese-Scott, C., Gonzales, N. R., Gwadz, M., Hao, L., He, S., Hurwitz, D. I., Jackson, J. D., Ke, Z., Krylov, D., Lanczycki, C. J., Liebert, C. A., Liu, C., Lu, F., Lu, S., Marchler, G. H., Mullokkandov, M., Song, J. S., Thanki, N., Yamashita, R. A., Yin, J. J., Zhang, D., and Bryant, S. H. (2007) *Nucleic Acids Res.* **35**, D237–D240
- Bendtsen, J. D., Nielsen, H., von Heijne, G., and Brunak, S. (2004) *J. Mol. Biol.* **340**, 783–795
- Emanuelsson, O., Nielsen, H., Brunak, S., and von Heijne, G. (2000) *J. Mol. Biol.* **300**, 1005–1016
- Krogh, A., Larsson, B., von Heijne, G., and Sonnhammer, E. L. (2001) *J. Mol. Biol.* **305**, 567–580
- Eisenhaber, B., Schneider, G., Wildpaner, M., and Eisenhaber, F. (2004) *J. Mol. Biol.* **337**, 243–253
- Kabsch, W., and Sander, C. (1983) *Biopolymers.* **22**, 2577–2637
- Jones, D. T. (1999) *J. Mol. Biol.* **292**, 195–202
- Simossis, V. A., and Heringa, J. (2005) *Nucleic Acids Res.* **33**, W289–W294
- Söding, J. (2005) *Bioinformatics* **21**, 951–960
- Zhu, B., Cai, G., Hall, E. O., and Freeman, G. J. (2007) *BioTechniques* **43**, 354–359
- Bills, C. E., McDonald, F. G., BeMiller, L. N., Steel, G. E., and Nussmeier, M. (1931) *J. Biol. Chem.* **93**, 775–785
- Pruess, L. M., Peterson, W. H., and Fred, E. B. (1932) *J. Biol. Chem.* **97**, 483–489
- Bell, A. A., Wheeler, M. H., Liu, J., Stipanovic, R. D., Puckhaber, L. S., and Orta, H. (2003) *Pest Manag. Sci.* **59**, 736–747
- Nielsen, N. J., Nielsen, J., and Staerk, D. (2010) *J. Agric. Food Chem.* **58**, 5509–5514
- Watanabe, A., Fujii, I., Sankawa, U., Mayorga, M. E., Timberlake, W. E., and Ebizuka, Y. (1999) *Tetrahedron Lett.* **40**, 91–94
- Watanabe, A., and Ebizuka, Y. (2002) *Tetrahedron Lett.* **43**, 843–846
- Chatterjee, S., and Mayor, S. (2001) *Cell. Mol. Life Sci.* **58**, 1969–1987
- Mayorga, M. E., and Timberlake, W. E. (1990) *Genetics.* **126**, 73–79
- Standforth, S. P. (2006) *Natural Product Chemistry at a Glance*, pp. 38–40, Wiley-Blackwell Publishing, Oxford
- Engh, I., Nowrousian, M., and Kück, U. (2007) *FEMS Microbiol. Lett.* **275**, 62–70
- Langfelder, K., Streibel, M., Jahn, B., Haase, G., and Brakhage, A. A. (2003) *Fungal Genet. Biol.* **38**, 143–158
- Jordan, D. B., Zheng, Y. J., Lockett, B. A., and Basarab, G. S. (2000) *Biochemistry* **39**, 2276–2282
- Basarab, G. S., Steffens, J. J., Wawrzak, Z., Schwartz, R. S., Lundqvist, T., and Jordan, D. B. (1999) *Biochemistry* **38**, 6012–6024
- Thompson, J. E., Basarab, G. S., Pierce, J., Hodge, C. N., and Jordan, D. B. (1998) *Anal. Biochem.* **256**, 1–6
- Marin, M., Heinz, D. W., Pieper, D. H., and Klink, B. U. (2009) *J. Biol. Chem.* **284**, 32709–32716
- Grocholski, T., Koskiniemi, H., Lindqvist, Y., Mäntsälä, P., Niemi, J., and Schneider, G. (2010) *Biochemistry.* **49**, 934–944
- Adams, M. A., and Jia, Z. C. (2005) *J. Biol. Chem.* **280**, 8358–8363
- Lee, W. C., Reniere, M. L., Skaar, E. P., and Murphy, M. E. (2008) *J. Biol. Chem.* **283**, 30957–30963
- Lemieux, M. J., Ference, C., Cherney, M. M., Wang, M., Garen, C., and James, M. N. (2005) *J. Struct. Funct. Genomics* **6**, 245–257
- Huber, O., and Sumper, M. (1994) *EMBO J.* **13**, 4212–4222
- Kawamoto, T., Noshiro, M., Shen, M., Nakamasu, K., Hashimoto, K., Kawashima-Ohya, Y., Gotoh, O., and Kato, Y. (1998) *Biochim. Biophys. Acta.* **1395**, 288–292
- Kim, J. E., Kim, S. J., Lee, B. H., Park, R. W., Kim, K. S., and Kim, I. S. (2000) *J. Biol. Chem.* **275**, 30907–30915
- Sato, K., Nishi, N., and Nomizu, M. (2004) *Arch. Biochem. Biophys.* **424**, 1–10
- Miyazaki, Y., Kaneko, S., Sunagawa, M., Shishido, K., Yamazaki, T., Nakamura, M., and Babasaki, K. (2007) *Curr. Genet.* **51**, 367–375
- Liu, T. B., Chen, G. Q., Min, H., and Lin, F. C. (2009) *J. Zhejiang Univ. Sci. B.* **10**, 434–444
- Pain, A., Woodward, J., Quail, M. A., Anderson, M. J., Clark, R., Collins, M., Fosker, N., Fraser, A., Harris, D., Larke, N., Murphy, L., Humphray, S., O’Neil, S., Perte, M., Price, C., Rabbinowitsch, E., Rajandream, M. A., Salzberg, S., Saunders, D., Seeger, K., Sharp, S., Warren, T., Denning, D. W., Barrell, B., and Hall, N. (2004) *Fungal Genet. Biol.* **41**, 443–453
- Hoppert, M., Gentzsch, C., and Schörgendorfer, K. (2001) *Arch. Microbiol.* **176**, 285–293
- Lendenfeld, T., Ghali, D., Wolschek, M., Kubicek-Pranz, E. M., and Kubicek, C. P. (1993) *J. Biol. Chem.* **268**, 665–671
- Evers, M. E., Trip, H., van den Berg, M. A., Bovenberg, R. A., and Driessen, A. J. M. (2004) *Adv. Biochem. Eng. Biotechnol.* **88**, 111–135
- van de Kamp, M., Driessen, A. J., and Konings, W. N. (1999) *Antonie Van Leeuwenhoek* **75**, 41–78
- Hong, S. Y., and Linz, J. E. (2008) *Appl. Environ. Microbiol.* **74**, 6385–6396
- Hong, S. Y., and Linz, J. E. (2009) *Mycol. Res.* **113**, 591–601
- Roze, L. V., Chanda, A., and Linz, J. E. (2011) *Fungal Genet. Biol.* **48**, 35–48
- Frandsen, R. J., Albertsen, K. S., Stougaard, P., Sørensen, J. L., Nielsen, K. F., Olsson, S., and Giese, H. (2010) *Eukaryotic Cell* **9**, 1225–1235